JOURNAL OF VIROLOGY, Apr. 2010, p. 3248–3258 Vol. 84, No. 7
0022-538X/10/$12.00 doi:10.1128/JVI.02155-09

Directional Spread of Surface-Associated Retroviruses Regulated by Differential Virus-Cell Interactions▽†

Nathan M. Sherer,[1]‡* Jing Jin,[2]‡ and Walther Mothes[2]

Department of Infectious Diseases, King's College School of Medicine, London SE1 9RT, United Kingdom,[1] and Section of Microbial Pathogenesis, Yale University School of Medicine, 295 Congress Avenue, New Haven, Connecticut 06536[2]

Received 12 October 2009/Accepted 11 January 2010

The spread of viral infections involves the directional progression of virus particles from infected cells to uninfected target cells. Prior to entry, the binding of virus particles to specific cell surface receptors can trigger virus surfing, an actin-dependent lateral transport of viruses toward the cell body (M. J. Lehmann et al., J. Cell Biol. 170:317–325, 2005; M. Schelhaas, et al., PLoS Pathog. 4:e1000148, 2008; J. L. Smith, D. S. Lidke, and M. A. Ozbun, Virology 381:16–21, 2008). Here, we have used live-cell imaging to demonstrate that for cells chronically infected with the gammaretrovirus murine leukemia virus in which receptor has been downregulated, a significant portion of completely assembled virus particles are not immediately released into the supernatant but retain long-term association with the cell surface. Retention can be attributed, at least in part, to nonspecific particle attachment to cell surface glycosylaminoglycans. In contrast to virus surfing, viruses retained at the surface of infected cells undergo a lateral motility that is random and actin independent. This diffusive motility can be abruptly halted and converted into inward surfing after treatment with Polybrene, a soluble cation that increases virus-cell adsorption. In the absence of Polybrene, particle diffusion allows for an outward flow of viruses to the infected cell periphery. Peripheral particles are readily captured by and transmitted to neighboring uninfected target cells in a directional fashion. These data demonstrate a surface-based mechanism for the directional spread of viruses regulated by differential virus-cell interactions.

Virus transmission from cell to cell critically contributes to the rapid spreading of viral infections (27). In the case of enveloped viruses, virus transmission generally involves an extracellular phase that is initiated by the budding and pinching off of viral particles from the producer cell prior to transmission to target cells and ends with cell entry by membrane fusion. The extracellular transmission phase can follow a cell-free mechanism, or, alternatively, the virus may be passed on at contacts established between infected and noninfected target cells. Strong evidence, particularly for retroviruses such as human immunodeficiency virus (HIV) and human T-cell leukemia virus (HTLV), points to a more efficient mode of transmission under conditions when cells directly contact each other (13, 16). Consistently, morphological studies indicate a strong accumulation of viral antigens and viral particles at the site of cell-cell contact (2, 13, 16, 19), and the direct transfer of viral particles has been directly documented in living cells (12, 30). Broad cell-cell contacts, designated virological synapses because of a resemblance to immunological synapses, as well as thin, filopodial or nanotube contacts have been described (8, 12, 14, 26, 30, 33). It has been suggested that an efficient coordination of assembly and entry at sites of cell-cell contact contributes to the overall efficiency of cell-to-cell transmission (15, 16, 23). Indeed, four-dimensional imaging of cell-to-cell transmission of murine leukemia virus (MLV) in living cells revealed that virus assembly can be polarized toward sites of cell-cell contact (14). In addition, uninfected cells may capture cell-free virus and pass it on to susceptible cells without themselves becoming infected. This pathway, first observed for HIV and dendritic cells, can facilitate efficient cell-to-cell transfer of surface virus to susceptible T cells (3, 9, 19, 36).

Here, we provide details of a surface-based transfer mechanism that contributes to the directional cell-to-cell spread of MLV. Using live-cell imaging, we show that newly assembled virus particles can be retained at the plasma membrane of chronically infected fibroblasts in which receptor has been downregulated from the cell surface. Viruses retained at the cell surface exhibit a lateral diffusive motility, a behavior that we call virus "surfacing." Virus surfacing in the cell periphery provided for contact-mediated transmission to receptor-expressing cells. Our data suggest a general mechanism wherein differential virus-cell interactions occurring at the cell surface contribute to the vectorial spread of viral infection.

MATERIALS AND METHODS

Cell lines. Rat XC sarcoma cells were cultured in modified Eagle's medium (MEM; Invitrogen) containing 10% fetal bovine serum (FBS) plus penicillin-streptomycin-glutamine. HEK293 cells used for virus generation were cultured in high-glucose Dulbecco's modified Eagle's medium (DMEM; Invitrogen) with 10% FBS plus penicillin-streptomycin-glutamine. XC cell lines stably expressing the ecotropic MLV receptor mCAT1 fused to cyan fluorescent protein (CFP) or yellow fluorescent protein (YFP) have been previously described (30). Infected XC cell lines were established by infection with Moloney MLV NCS-FLAG (Moloney MLV carrying a FLAG epitope tag in the p12 domain of Gag) (37) added in the presence of 5 μg/ml Polybrene and cultured for 14 days to establish a chronic infection. At 14 days postinfection, cells were trypsinized, washed with phosphate-buffered saline (PBS), and incubated for 30 min with 100 nM fluo-

* Corresponding author. Mailing address: Department of Infectious Diseases, King's College London School of Medicine, 2nd floor, Borough Wing, Guy's Hospital, London Bridge, London SE1 9RT, United Kingdom. Phone: (44) 20 718 85398. Fax: (44) 20 718 83385. E-mail: nathan.sherer@kcl.ac.uk.

‡ N.M.S. and J.J. contributed equally to this work.

† Supplemental material for this article may be found at http://jvi.asm.org/.

▽ Published ahead of print on 20 January 2010.

rescein isothiocyanate (FITC)-labeled soluble receptor binding domain (RBD) of the Friend murine leukemia virus (a generous gift from David Wensel and James Cunningham, Harvard Medical School, Boston, MA) (1, 4) prior to flow cytometry using a FACSCalibur (Becton-Dickinson) in order to measure mCAT-1 surface expression (see Fig. 2A and B). For marker transduction, infected or uninfected XC cells were infected with inactivated vector viruses encoding the fluorescently tagged proteins as described below.

Plasmids and vector virus generation. Moloney MLV (NCS-FLAG) stocks were generated by transient transfection of HEK293 cells with plasmid pNCS-FLAG encoding a molecular clone of Moloney MLV carrying a FLAG tag inserted into the p12 domain of Gag (a kind gift of Steve Goff, Columbia University, New York, NY) (37). Lentivirus stocks encoding MLV Gag-CFP/YFP and MLV Env-YFP were generated using plasmids of the HELIX transduction system (a kind gift of Gary Nolan, Stanford University, Palo Alto, CA). To generate HELIX Gag-CFP/YFP and MLV Env-YFP, the coding regions of Gag-CFP/YFP and MLV Env-YFP were PCR amplified from plasmids pGag-CFP/YFP and Env-YFP (31) and cloned into packaging vector HELIX-CS. The MLV-based vector encoding YFP-actin was a kind gift of Johannes Huppa (Stanford University, Palo Alto, CA). YFP-actin-expressing virus was generated by cotransfection of HEK293 cells with MLV Gag-Pol and MLV Env plasmids as previously described (31). All viruses were generated by transient transfection of HEK293 cells using FuGene 6 reagent (Roche) according to the manufacturer's specifications. Supernatants were harvested at 24 and 48 h posttransfection, filtered through 0.2-μm-pore-size filters (Millipore), and used directly for infection or transduction or stored frozen at −80C.

Live imaging and cellular manipulation. Live-cell imaging was performed at 37°C by using a 60× oil objective (numerical aperture, 1.4) of a Nikon TE2000 inverted wide-field microscope equipped with Piezo drive or by using an Improvision spinning disc confocal microscope equipped with a Nikon TE2000 base as previously described (14, 30). Cells were plated on 35-mm imaging dishes (MatTek, Ashland, MA) coated with poly-L-lysine or fibronectin in MEM with 10% FBS plus penicillin-streptomycin-glutamine as previously described (30). Time-lapse acquisition of CFP or YFP channels was every 4 to 60 s, as indicated in the legends to the supplemental movies. Fibronectin, cytochalasin D, nocodazole, sodium azide, Polybrene, and heparinase II were obtained from Sigma-Aldrich (St. Louis, MO). Drugs were administered at the concentrations indicated in the figure legends by 10-fold dilution into the culture medium during live-cell imaging. Exogenously administered fluorescent viruses (see Fig. 6 and 7) were generated as previously described (18), diluted in MEM containing 10% FBS, and added directly to the culture medium. Coculturing of producer and target cells to monitor viral spread (see Fig. 7) was as previously described (14, 30). All imaging experiments were carried out a minimum of three times in order to confirm reproducibility. Endogenous Gag fluorescence was pseudo-colored green, and additional markers or exogenously administered viruses were pseudo-colored red. All movies were edited using Openlab (PerkinElmer) and ImageJ (NIH) software packages and saved for presentation in Quicktime format using Sorensen 3 compression. Single-particle tracking was performed using Openlab or Volocity software packages (PerkinElmer). Particle assembly was monitored as previously described (14). The first peak of fluorescence achieving 85% of maximum intensity was chosen as a threshold representing the completion of particle assembly (defined as time [*T*] zero). Relative position and velocity were calculated for particle movements to or from the cell body as previously described (30).

Virus adsorption assay. XC cells chronically infected with MLV (XC-MLV) were seeded on glass coverslips for 24 h prior to the addition of Gag-YFP-labeled MLV viruses to the culture supernatant in the absence or presence of 5 μg/ml Polybrene at 37°C. At select time points after Polybrene addition, cells were washed three times with ice-cold PBS prior to fixation with 4% paraformaldehyde. Images were acquired using an Improvision spinning disc confocal microscope equipped with a Nikon TE2000 base and analyzed using Volocity software (PerkinElmer). Virus adsorption was measured by quantifying the total number of fluorescent particles bound to cells per imaging area (~13 cells over 7.28 mm^2) and averaged over three experiments.

RESULTS

Newly assembled viruses can be retained at the surface of the infected cell. The visualization of *de novo* MLV assembly using spinning disc confocal microscopy revealed a large number of viral particles that remained associated with the plasma membrane of producer cells after the completion of assembly (Fig. 1; see also Movie S1 in the supplemental material). Rat XC cells chronically infected with ecotropic MLV (XC-MLV cells) were plated on glass coverslips, transiently transfected with plasmids expressing MLV Gag-YFP, and imaged at ~24 h posttransfection. Nascent virions, defined as fluorescent dots that appeared at the cell surface and intensified over time, were monitored using spinning disc confocal microscopy as previously described (Fig. 1A and B; see also Movie S1) (14). Similar to previous observations of HEK293 and Cos-1 cells, two distinct fates of *de novo* appearing fluorescent particles were detected in XC-MLV cells (14). First, following the completion of assembly, particles disappeared, which is consistent with rapid release into the culture supernatant (Fig. 1C). Second, a significant portion of viral particles (~30%) remained associated with cells for prolonged periods of time after achieving threshold fluorescence intensity (Fig. 1D). Remarkably, retention times of >60 min were frequently observed for individual particles (Fig. 1D).

MLV surfacing on chronically infected cells. To reliably monitor virus particles in the context of a spreading infection, we established chronically infected XC cell lines that stably generated fluorescently labeled MLV virions. Cells were infected with ecotropic MLV (Moloney MLV NCS-FLAG, carrying a FLAG epitope tag in the p12 domain of Gag [37]) and cultured for at least 14 days. After 14 days, viral infection led to the downregulation of the MLV receptor mCAT-1, as verified by flow cytometry using the FITC-labeled receptor binding domain (RBD) of the ecotropic MLV envelope protein as a probe (1, 4) (Fig. 2A and B). Viral particles were visualized by transducing XC-MLV cells with lentiviruses encoding MLV Gag-CFP alone or in combination with lentiviruses encoding MLV Env-YFP (Fig. 2C). Indirect immunofluorescence using an anti-FLAG antibody confirmed similar distributions of Gag-positive puncta in XC-MLV cells not transduced to express Gag-CFP; and after Gag-CFP transduction, the majority of CFP-positive particles were coincident with FLAG-tagged Gag, suggesting heterooligomerization of Gag-FLAG and Gag-CFP molecules (data not shown). Importantly, cotransduction of Gag-CFP with Env-YFP resulted in an enrichment of Env-YFP at Gag-CFP-positive puncta, demonstrating that these particles were enveloped at the cell surface, which is consistent with infectious virus production (Fig. 2C).

Live-cell imaging using wide-field fluorescence microscopy revealed a static population of particles apparently released and immobilized against the glass coverslip (Fig. 3A, yellow arrows) and a motile, cell-associated population demonstrating dramatic movements predominately at the cell periphery, in many instances projecting outward from the cell surface (Fig. 3A, green arrows; see also Movie S2 in the supplemental material). Single particles were tracked migrating across the actin-rich cell periphery (visualized using YFP-actin), the lamellum, the lamellar edge, or moving up and down the lengths of filopodia or retraction fibers (Fig. 3A, white traces, and Movie S2). Particles exhibited rapid multidirectional movements averaging 9.18 μm/min (± 5.8; $n = 10$) with frequent "jumps" occurring at rates up 40 μm/min (Fig. 3B, left panels). Unlike with virus surfing motility that proceeds inward during virus entry (18, 28, 32), there was no directional bias inward or outward (Fig. 3B, left panels). Even though particle motility was observed on peripheral actin-rich structures, treating cells

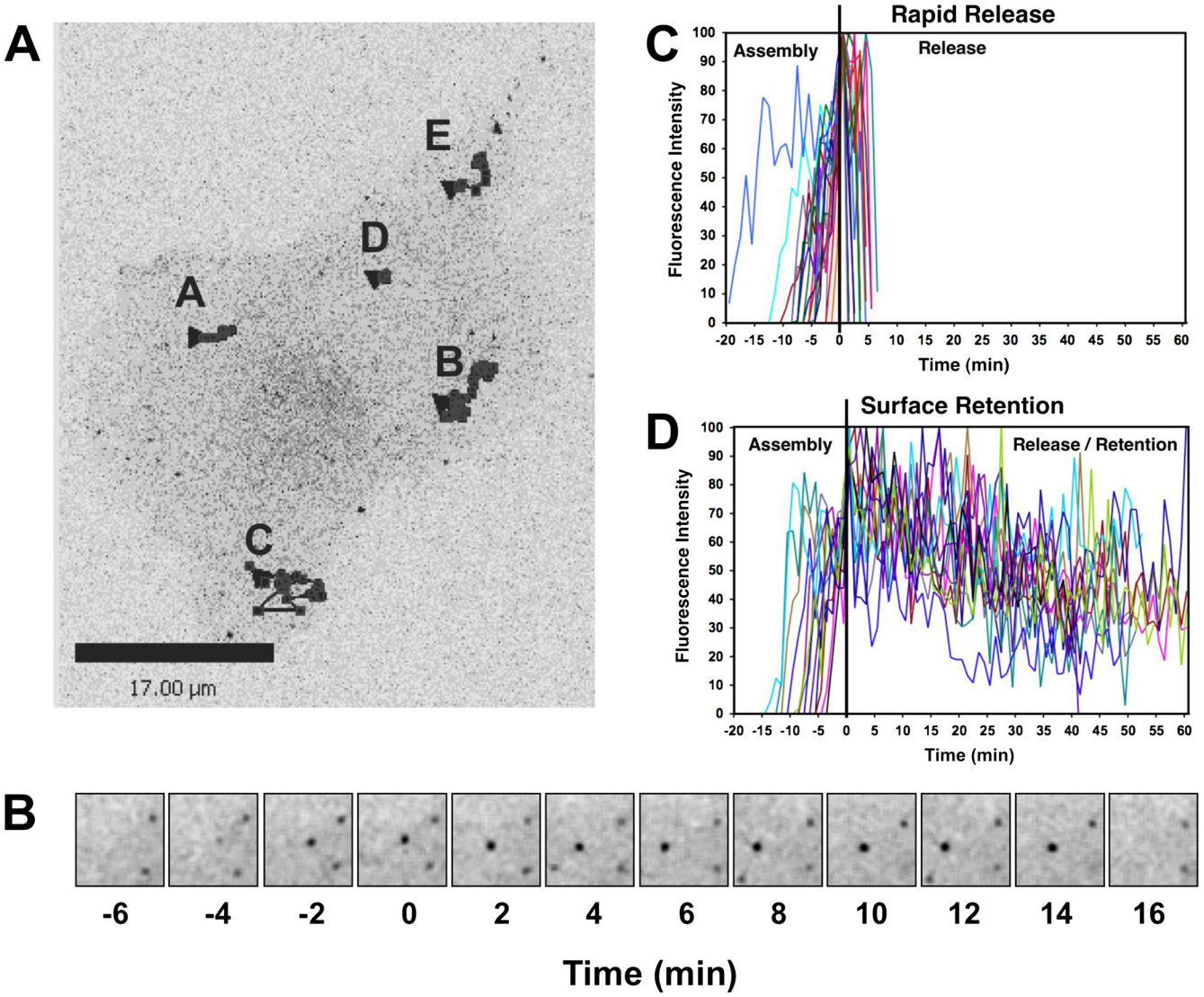

FIG. 1. Newly assembled MLV particles can be retained at the infected-cell surface. (A) MLV-infected fibroblasts (XC-MLV cells) were plated on glass coverslips, transfected to express MLV Gag-YFP, and imaged 24 h posttransfection using spinning disk confocal fluorescence microscopy. Shown is the final frame from Movie S1 in the supplemental material. Stacks were acquired at ~1-min intervals over ~2.5 h. Black traces represent the movement of several particles that appeared *de novo* and were tracked throughout the length of the experiment. Size bar, 17 μm. (B) The assembly and release of a representative particle (particle A) from the experiment described in panel A. Time zero ($T = 0$) is the time at which the particle achieved threshold fluorescence (as described in Materials and Methods), representing the completion of virus assembly. Each square represents ~49 μm^2. (C and D) Changes in fluorescence intensity over time for *de novo* assembling particles tracked for the experiment described in panel A. After reaching threshold intensity ($T = 0$), particle fluorescence disappeared within 10 min for the majority of particles (C) while ~30% of the particles could be monitored at the cell surface for an extended period of time (D).

with 5 μM cytochalasin D, an actin depolymerization reagent, for 5 (Fig. 3B, right panels) or 60 min (see Fig. 5C and D and Movie S5) had little effect on particle motility on the lamellum (particle rate of 10.79 ± 7.65 μm/min; $n = 11$) (Fig. 3B, right panels). Treatment with 10 mM sodium azide, an inhibitor of cellular ATPases, or 5 μM nocodazole, a reagent that depolymerizes microtubules, also had no discernible effect on surface motility (data not shown). In sum, these data suggested that surface-retained particles frequently exhibit a lateral motility that is actin independent and driven by diffusion. Because this behavior was distinct from the inward, actin-dependent surfing observed during viral entry into receptor-expressing cells, we called this motility virus "surfacing." Interestingly, in contrast to the outward migration reported for gold beads near the leading edge of the neuronal growth cone (29), virus surfacing was not actin dependent.

A role for cell surface GAGs in virus particle retention. Retroviruses including MLV and HIV are able to bind to cells through interactions with cell surface glycosaminoglycans (GAGs) (34, 35), notably heparan sulfate (7, 11), even in the absence of specific viral receptor molecules. To test if the retention and motility of assembled viruses at the infected-cell surface reflected an association with GAGs, we initiated live-cell imaging prior to the addition of heparinase II, which cleaves heparan

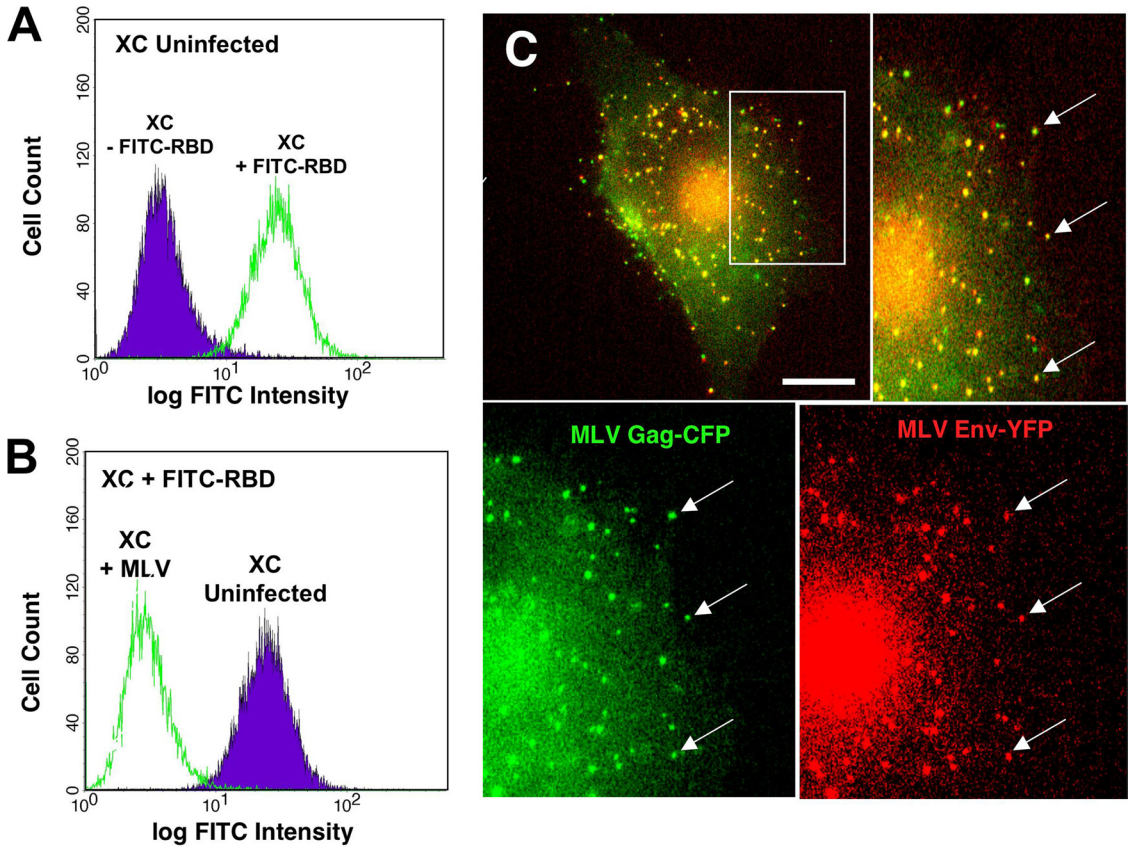

FIG. 2. XC-MLV cells. (A and B) Receptor mCAT-1 is downregulated from the surface of chronically infected XC-MLV cells. Uninfected and infected rat XC cells were fixed and stained with FITC-labeled receptor-binding domain (RBD), an MLV Env-based probe that specifically binds to receptor mCAT-1, prior to washing and analysis by flow cytometry to measure receptor levels on the cell surface. (A) Uninfected XC cells stained with (green) or without (purple) FITC-RBD to confirm probe specificity. (B) XC cells infected with ecotropic MLV (green) or not infected (purple) were cultured for 14 days prior to staining with FITC-RBD. (C) Chronically infected XC-MLV cells stably expressing Gag-CFP (green) and Env-YFP (red) were plated on glass coverslips prior to live-cell imaging. The arrows indicate enrichment of the surface Env-YFP protein on bright Gag-CFP-positive puncta.

sulfate, to the cell culture medium. Treatment with heparinase II led to the disappearance of a subset of surfacing virus particles, consistent with particle release into the cell supernatant (Fig. 4 and Movie S3 in the supplemental material). This result was consistent with a role for GAGs, at least in part, in retaining particles at the cell surface. Previously it was demonstrated that infection by HIV-1 is promoted by GAGs on target cells but only for HIV-1 isolates carrying a viral Env protein with a highly positively charged V3-loop (38). In our system, we observed virus surfacing even for cells generating Gag-CFP in the absence of MLV Env (data not shown), consistent with the notion that MLV's association with GAGs or alternative receptors on infected XC cells is not necessarily Env dependent (11, 24, 25, 35).

Polybrene treatment switches surfacing to surfing on infected cells. We hypothesized that surfacing motility reflected a relatively weak association between virus particles and nonspecific receptor molecules such as GAGs on the infected-cell surface, in contrast to the more specific association formed between virus and mCAT-1 receptor molecules after binding to an uninfected target cell. We attempted to influence this interaction by adding Polybrene, a soluble cationic molecule that neutralizes otherwise repulsive negative membrane charges, to the culture medium of XC-MLV cells generating Gag-CFP labeled viral particles. Treatment with Polybrene has been demonstrated to substantially increase the adsorption of MLV to the cell surface (5, 6) and is commonly used to improve viral infectivity. We initiated live-cell imaging of XC-MLV cells expressing Gag-CFP for 10 min prior to the addition of Polybrene. Strikingly, the addition of Polybrene completely abrogated random particle motility at the cell surface (Fig. 5A and B; see also Movie S4 in the supplemental material). In fact, a brief lag period was followed by uniform particle transport inward with accumulation at or near the rounded cell body. Inward trafficking proceeded at $0.472 \pm 0.149 \mu m/min$ ($n = 32$), a rate consistent with engagement of retrograde actin flow, as we have previously described for receptor-dependent virus surfing on uninfected target cells (18). Indeed, the effects of Polybrene were clearly actin dependent. Pretreatment with 20 μM cytochalasin D (Fig. 5C and D; see also Movie S5) and 10 mM sodium azide (data not shown) completely abolished inward surfing after Polybrene treatment. Instead of surfing inward, particles became frozen and remained static for the remainder of the imaging period. In these experiments, disruption of the actin cytoskeleton after cytochalasin D treatment was confirmed by monitoring YFP-

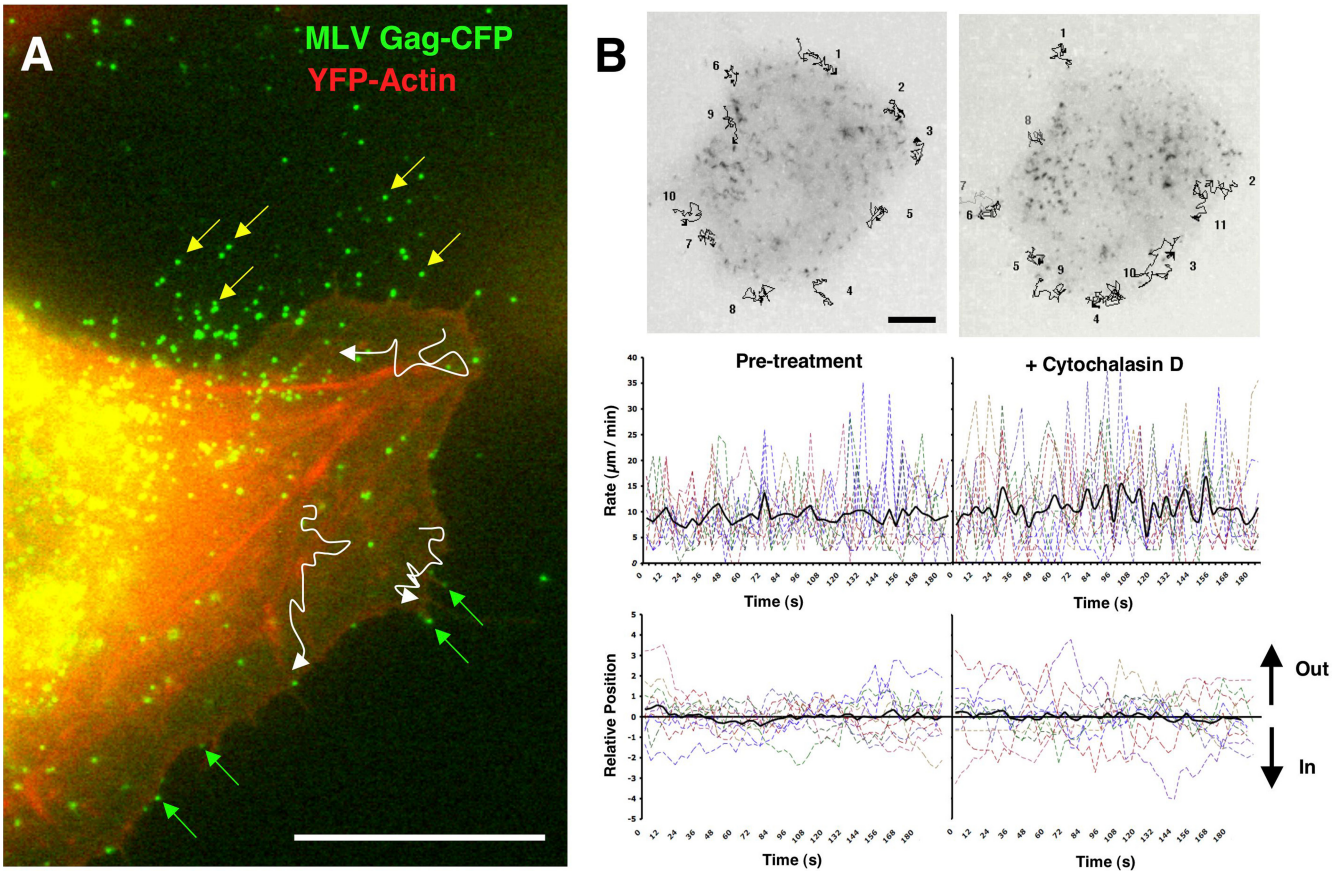

FIG. 3. Surfacing motility on the plasma membrane of the infected cell. (A) XC-MLV cells were transduced with Gag-CFP and YFP-actin prior to monitoring fluorescent particle motility by live-cell imaging. Figure corresponds to Movie S2 in the supplemental material. White traces represent virus particle trajectories across the lamellum over ~20 min. Green arrows indicate virus particles associated with the actin-rich cell periphery, the filopodia, or the edge of the cell lamellum. Yellow arrows indicate virus particles shed from the cell surface and adhered to the glass coverslip. (B) An experiment as in panel A in which Gag-CFP particle motility was monitored before and after the addition of 5 μM cytochalasin D to the culture medium. Images represent an overlay of ~35 frames acquired over ~180 s. Black lines represent trajectories for 11 particles monitored before and after cytochalasin D treatment. Particle rates (μm/min) and positions relative to the edge of the cell are plotted below. Black lines represent the average values for 11 particles. Size bar, 10 μm.

actin (Fig. 5C, lower panels). We speculate that the abrupt immobilization of particles after sequential cytochalasin D and Polybrene treatments reflects the formation of a transmembrane anchorage between each virus on the outer surface of the cell and the actin cytoskeleton that underlies the plasma membrane. Treatment with cytochalasin D blocked retrograde F-actin flow (18, 20) and therefore abolished inward movement.

Exogenously bound viruses exhibit similar behaviors on the infected-cell surface. If surfacing represents a nonspecific association of assembled viruses with the infected-cell surface, then exogenously bound viruses should also be bound and exhibit similar lateral behaviors. To test this notion, we transiently transfected HEK293 cells to generate Gag-YFP-labeled MLV virions. Viral supernatants were purified using 0.45-μm-pore-size filters and concentrated by centrifugation through a 20% sucrose cushion. We have previous demonstrated that these viruses retain a high degree of infectivity and undergo virus surfing in a receptor-dependent fashion after binding to uninfected target cells (18). We added Gag-YFP-labeled MLV to the culture medium during live-cell imaging of XC-MLV cells, generating Gag-CFP-labeled particles (Fig. 6A and B; see also Movie S6 in the supplemental material). Exogenously added Gag-YFP particles were readily bound to the surface of infected cells, and numerous instances of random motility consistent with virus surfacing were detected, with some observations of directional inward motility (Fig. 6A and B and Movie S6). Again, the addition of Polybrene abolished all random flux. All particles, exogenously administered (Gag-YFP-labeled) or endogenously generated (Gag-CFP-labeled), surfed inward toward the cell body (Fig. 6A and B and Movie S6).

We sought to verify that Polybrene treatment was indeed affecting virus-cell adsorption in our system. To this end, Gag-YFP-labeled MLV particles were added to cultures of confluent XC-MLV cells in the presence or absence of 5 μg/ml Polybrene and incubated at 37°C for 5, 10, 30, or 60 min prior to fixation. Three-dimensional (3D) representations were generated from stacks acquired using a spinning disk confocal microscope (Fig. 6C), and virus adsorption was quantified by counting the number of cell-associated fluorescent particles bound over equal areas of each coverslip (~13 cells per 7.3 mm^2) (Fig. 6D). MLV Gag-YFP particles added exogenously

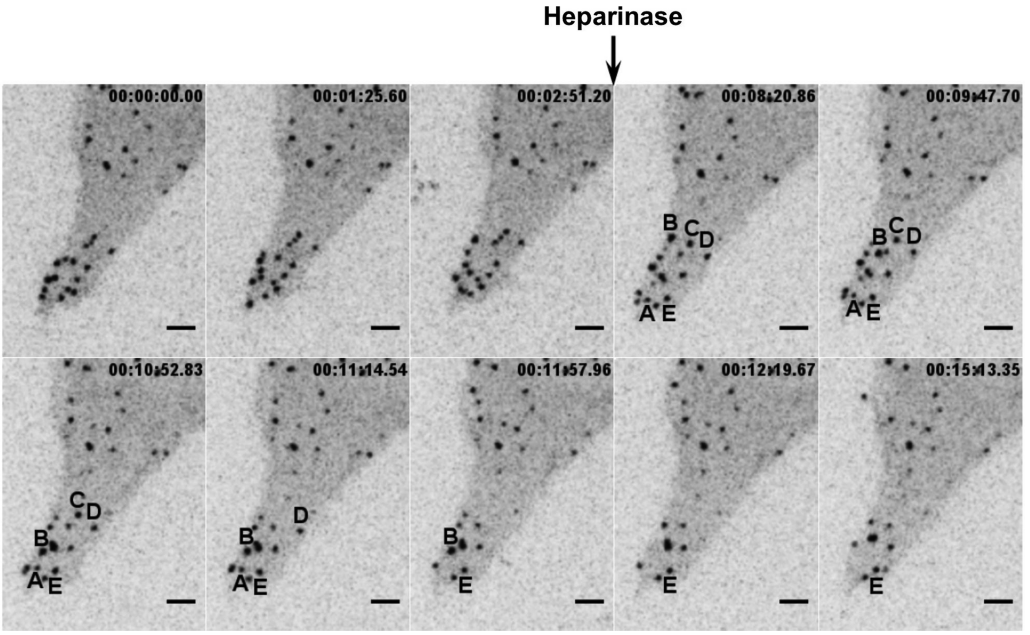

FIG. 4. Surfacing viruses are released after treatment with heparinase. XC-MLV cells transduced to express MLV Gag-CFP were plated on glass coverslips for 24 h prior to live-cell imaging before and after treatment with heparinase. Individual frames from time-lapse acquisition are shown. The black arrow indicates the time point at which 5 U/ml heparinase II was added to cells. Five representative particles (A to E) were tracked after heparinase treatment. Particles A to D disappeared, and particle E remained associated with the cell throughout the duration of the experiment. The corresponding time lapse is presented as Movie S3 in the supplemental material. Size bar, 5 μm.

were readily bound to infected cells under either condition, but the addition of Polybrene significantly enhanced virus adsorption to the cells at every time point. Taken together, these data confirmed that MLV-infected cells can bind and retain cell-free virus particles even in the absence of functional receptor. Polybrene treatment affected endogenously generated and exogenously added viruses identically, establishing a correlation between virus-cell adsorption and the inward surfing motility triggered on the infected-cell surface.

Receptor binding during directional cell-to-cell spread triggers a switch from surfacing to surfing behavior. We previously reported the cell-to-cell spread of viruses across filopodial bridges we termed viral cytonemes (30). Cell-cell contact between receptor-expressing target cells and virus-infected cells leads to cytoneme formation. This process is dependent on the interaction between the receptor on the target cell surface and the viral Env protein on the infected-cell surface and requires a functional actin cytoskeleton. Here, we asked if retained, surfacing viruses were accessible cargoes competent for cell-to-cell transmission. To visualize intercellular interactions between infected producer and uninfected receptor-expressing target cells, we added XC-MLV cells generating Gag-CFP to cultures of uninfected target XC cells stably expressing the YFP-labeled ecotropic MLV receptor mCAT-1 (Fig. 7A B; see also Movie S7 in the supplemental material). Cells were allowed to settle onto the coverslip for 2 to 6 h prior to time-lapse imaging. In the absence of target cells, virus particles surfaced and accumulated in the cell periphery (Fig. 7A and B, particle C; see also Movie S7). However, once a contact was established, surfacing particles contacting the receptor-rich filopodium ceased random movement. These particles were pulled away from the infected cells and began to undergo unidirectional transport, surfing along the filopodium and lamellipodium toward the cell body of the target cell (Fig. 7A and B, particles A, B, and D; see also Movie S7).

As a further test we prebound Gag-CFP-labeled MLV particles to XC-MLV cells expressing Gag-YFP prior to coculture with uninfected XC target cells expressing mCAT-1-CFP (Fig. 7C and D; see also Movie S8 in the supplemental material). Both endogenously generated Gag-YFP particles and exogenously bound Gag-CFP particles were observed to migrate across the same filopodial bridge (Fig. 7C and D, green endogenous particles A and B and red prebound particle A; see also Movie S8). In sum, peripherally localized surfacing viruses are competent for transmission at sites of cell-cell contacts. Furthermore, specific virus-receptor interactions are sufficient to transition virus surfacing into virus surfing, establishing the unidirectional, actin-driven transfer of viruses from cell to cell.

DISCUSSION

Herein, we have described the behavior of MLV particles that are retained at the infected-cell surface after the completion of assembly and are competent for subsequent transmission to uninfected target cells after establishing a physical cell-cell interface. Several observations convinced us that these surfacing particles represented fully assembled viruses retained at the cell surface. First, 4D imaging demonstrated a subpopulation of MLV particles that remain associated with the plasma membrane after reaching maximum fluorescence (Fig. 1). These particles are likely completely assembled because they often begin to undergo diffusive movement soon after reaching maximum fluorescence (14). Second, these particles successfully recruited MLV Env-YFP glycoproteins,

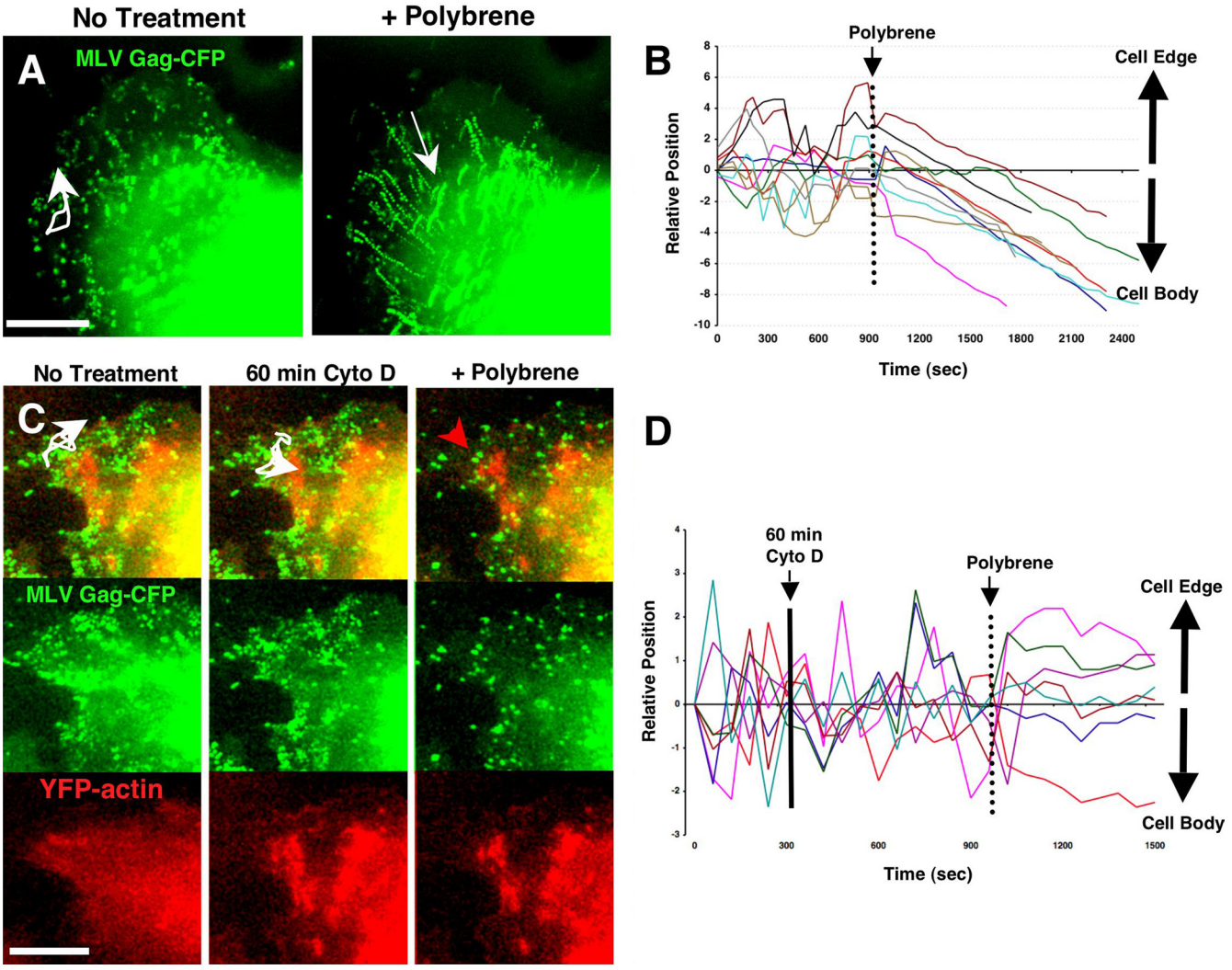

FIG. 5. Polybrene abolishes surfacing and triggers actin-dependent surfing on the infected-cell surface. (A) XC-MLV cells transduced to express MLV Gag-CFP were plated on glass coverslips and imaged for several minutes prior to the addition of 5 μg/ml Polybrene. Images represent superimposed frames from 10 min of live-cell imaging before and after Polybrene addition. The corresponding time lapse is presented as Movie S4 in the supplemental material. White arrows indicate selected individual particle trajectories over time. (B) The positions of particles relative to the cell body were tracked before and after Polybrene addition for the experiment described in panel A. (C) An experiment as in panel A for XC-MLV cells transduced to express both Gag-CFP and YFP-actin (red). Cells were imaged for several minutes prior to treatment for 60 min with 20 μM cytochalasin D to depolymerize the actin cytoskeleton. Cells were then imaged for several more minutes prior to the addition of 5 μg/ml Polybrene. White traces indicate individual particle trajectories prior to Polybrene treatment. The red trace indicates a Gag-CFP particle immobilized after the combined cytochalasin D and Polybrene treatments. An alternative region of interest from the same experiment is presented as Movie S5 in the supplemental material. (D) The positions of several particles from the experiment described in panel C were tracked relative to the cell edge or cell body before and after treatments with cytochalasin D and Polybrene. Size bar, 10 μm.

thereby demonstrating virus membrane envelopment (Fig. 2C). Third, surface-associated particles were competent for release from the cell surface and were transmitted to uninfected target cells at sites of cell-cell contacts (Fig. 7). Fourth, surfacing particles were affected by the administration of Polybrene (Fig. 5). Finally, exogenously added viruses could be bound and retained at the cell surface similarly to endogenously generated particles and exhibited similar surfacing and surfing behaviors (Fig. 6).

The nonspecific absorption of MLV to target cells has been described for a variety of cell types and is at least partially attributed to associations with GAGs (11, 24, 25, 35). A subpopulation of surfacing particles can be released from the cell surface of producer cells after treatment with heparinase, suggesting that heparan sulfate contributes to the observed retention of viruses on infected cells. Because surface-associated viruses are efficiently transferred to uninfected target cells, we perceive plasma membrane retention as a potential mechanism by which viruses promote their cell-to-cell spread. Nonspecific cell surface proteins as well as specific C-type lectins have also been implicated in HIV-1 adsorption and spread, most notably in the transfer of HIV from dendritic cells to T cells (9, 19). Our data suggest that GAGs could play a similar role in many cell types.

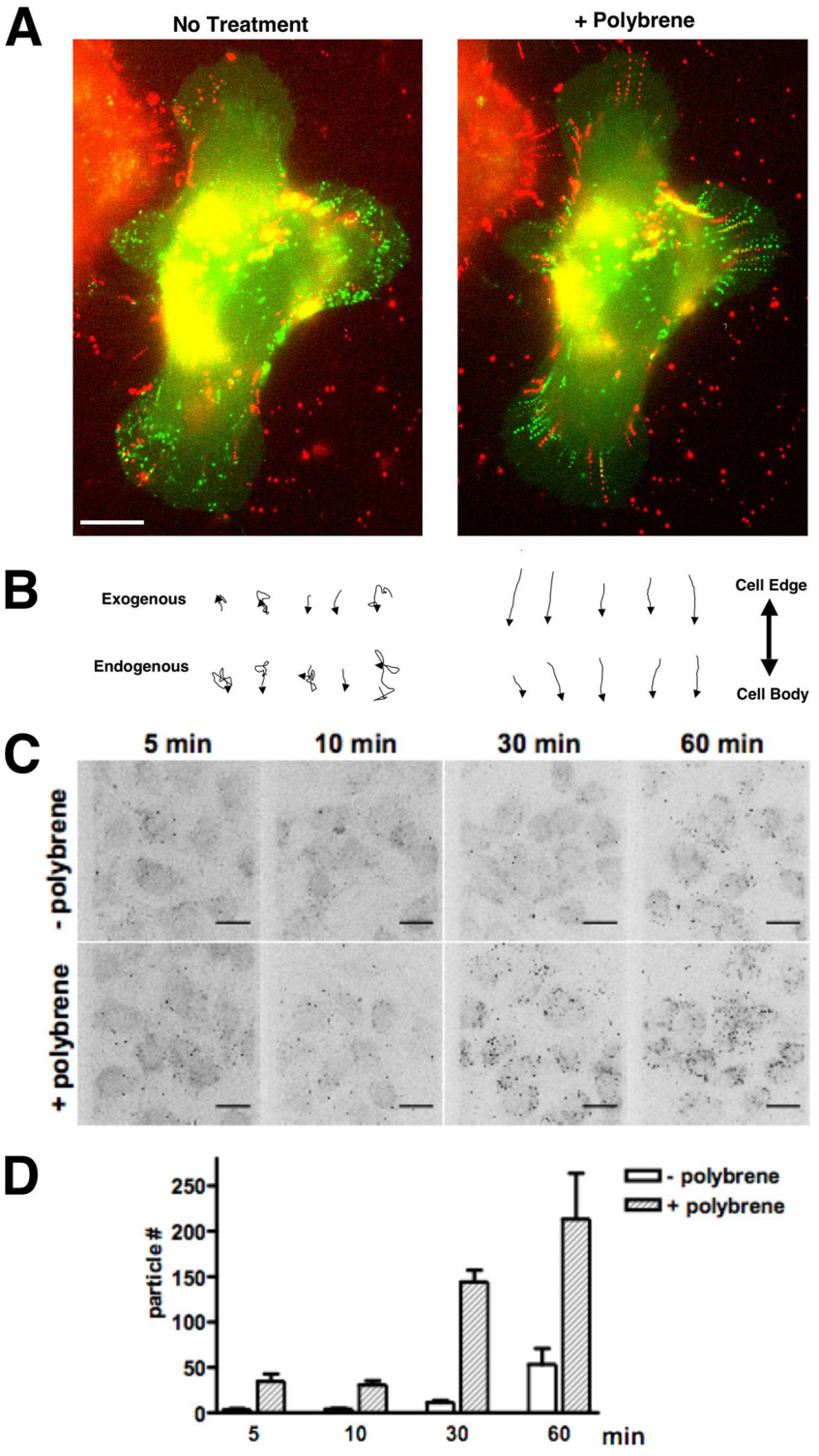

FIG. 6. Polybrene-induced surfing on infected cells correlates with an increase in virus adsorption to the cell surface. (A) Exogenously added virus particles are bound to the infected cell and undergo surfacing and surfing behaviors similar to endogenously generated virus particles. MLV particles labeled with Gag-YFP (red) were added to a culture of XC-MLV cells expressing Gag-CFP (green). Imaging was initiated shortly after the addition of exogenous virus, and images were collected for several minutes prior to (left panel) and after (right panel) the addition of 5 μg/ml Polybrene. Shown are composite images combining all frames from the time-lapse movie either before or after the addition of Polybrene. The figure corresponds to Movie S6 in the supplemental material. (B) Individual traces for several particles, either exogenously bound (top) or endogenously generated (bottom), tracked during the experiment described in panel A for 10 min before (left) or after (right) Polybrene addition. Traces have been orientated based on their trajectory toward or away from the cell body, as indicated on the right. Size bar, 10 μm. (C) Polybrene treatment enhances MLV adsorption to the infected-cell surface. XC-MLV cells plated on glass coverslips were incubated with Gag-YFP labeled MLV particles for the time indicated prior to fixation, image acquisition, and generation of 3D reconstructions. (D) Virus adsorption was measured by quantifying the total number of particles bound to cells on equal areas of each coverslip (~13 cells over 7.27 mm^2) for the experiment described in panel C. Error bars represent the standard deviation over three experiments.

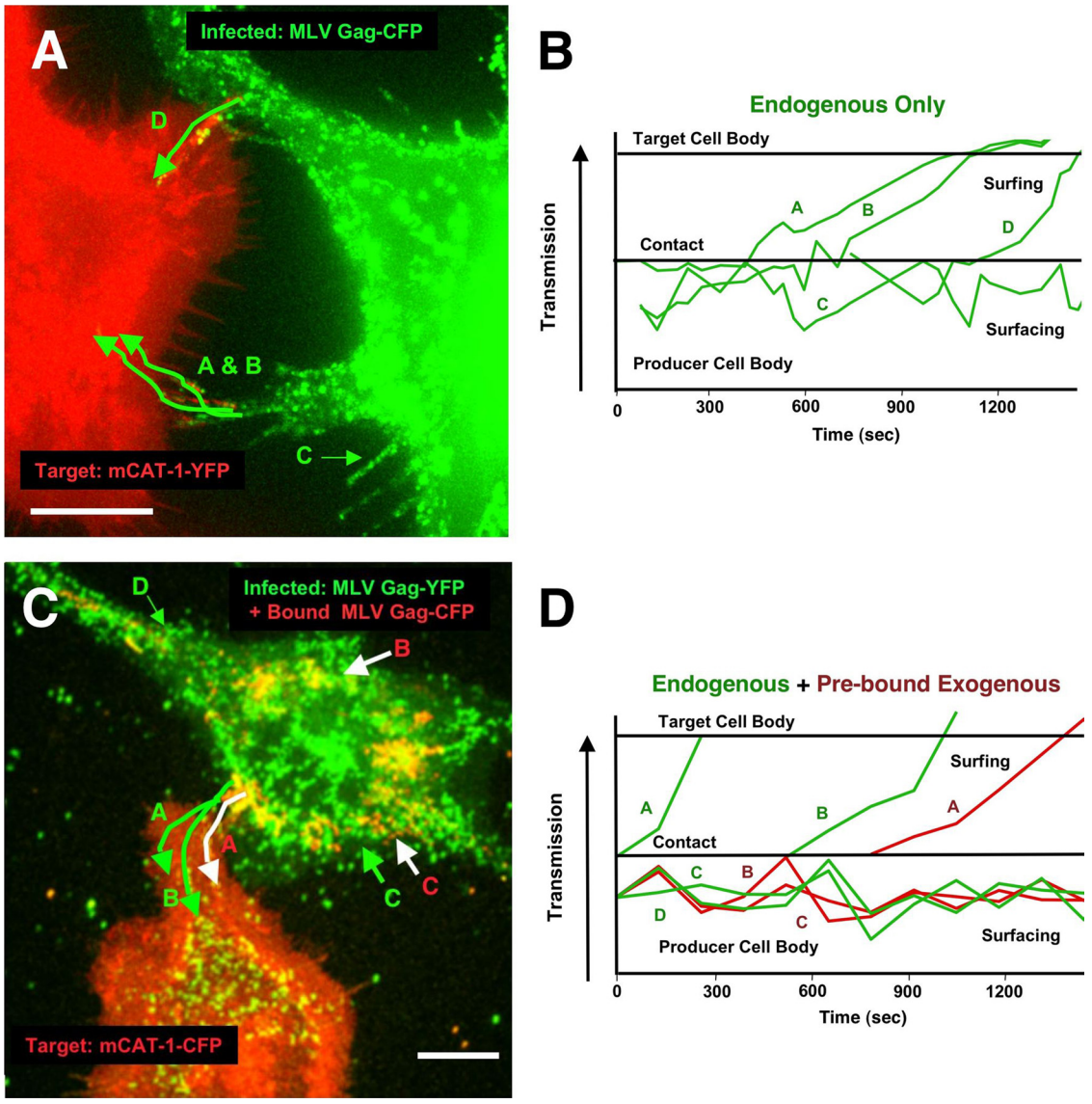

FIG. 7. Surfacing viruses are competent for cell-cell transmission regulated by virus-receptor binding. (A) XC-MLV cells expressing Gag-CFP (green) were coincubated with uninfected XC cells expressing mCAT-1-YFP (red) on glass coverslips and subjected to live-cell imaging. The figure corresponds to Movie S7 in the supplemental material. The image is an overlay of frames from ~90 min of acquisition. Green traces indicate the trajectories of selected particles A to D over time. (B) The positions of selected particles A to D relative to the infected-cell body were tracked over time. Particles A, B, and D represent surfacing particles that are accessed by the target cell and transferred directionally from cell to cell. Particle C is a surfacing particle that is not transferred during the experiment. (C) Cell-free Gag-YFP-labeled MLV particles (red, top cell) were prebound to infected XC-MLV cells expressing Gag-CFP (green) prior to coincubation with cells expressing mCAT-1-YFP (red, lower cell) on glass coverslips and live-cell imaging. The figure corresponds to Movie S8 in the supplemental material. Shown is an overlay of frames from ~30 min of imaging. Green traces indicate cell-cell transfer for two endogenously generated Gag-CFP-labeled particles (particles A and B in green). A white trace indicates cell-cell transfer of an exogenously added Gag-YFP-labeled particle (particle C in red). (D) The positions of select particles highlighted in panel C were tracked relative to the infected-cell body over time. Size bar, 10 μm.

The discovery of the antiviral factor tetherin reinforces the importance of a surface-associated intermediate in the retroviral life cycle following the completion of assembly that can be targeted by antiviral factors (21, 22). Tetherin can sequester newly assembled enveloped virus particles on the cell surface of infected cells, thereby preventing their release (10, 17). HIV-1 counters tetherin activity by expressing the viral accessory protein Vpu. Importantly, whether surface-retained, "tethered" HIV-1 lacking Vpu is still competent for cell-to-cell spread remains to be fully addressed. Virus surface sequestration may be either beneficial (e.g., dendritic cell [DC]-based *trans*-infection; also this report) or detrimental (e.g., tetherin-based restriction) to viral replication. Interestingly, expression of tetherin in MLV-expressing cells led to an immobilization of surface-associated MLV, preventing the diffusive movement of MLV described here (J. Jin and W. Mothes, unpublished results). Thus, endogenous rat tetherin likely does not play a role in the surfacing behavior we have described on XC cells.

Our studies imply a model for virus spread in which receptor downregulation would serve as an elegant viral strategy for establishing a polarized gradient for the flow of viruses from infected to uninfected cells. First, the replacement of functional receptor molecules at the cell surface with the virally encoded Env glycoproteins establishes an infected cell as competent to bind with high avidity to uninfected target cells expressing cognate receptor molecules. Second, the concomitant reduction of virus-cell interactions on the infected-cell surface due to receptor downregulation promotes outward release and/or surfacing of nascent virions, wherein viral diffusion can proceed until particles are shed or "passed on" at cell-cell contacts. Virus-receptor binding confers directional actin-based surfing motility and hence results in a polarized flow of viruses from infected cells to uninfected target cells. We have previously demonstrated that virus surfing precedes entry and, therefore, a signal is necessarily transmitted to engage the underlying actin flow at receptor binding (18). Polybrene induction of surfing even on infected cells suggests that it may be the strength of the virus-cell interaction and not necessarily the specificity of the interaction that initiates virus surfing. However, for the spreading of viral infection in the absence of Polybrene, the specific match between Env and receptor is all that is necessary as a trigger for directional viral transport from cell to cell (30).

Finally, our data suggest that surfacing viruses may represent a reservoir of infectious virus particles that can be sequestered and later passed on to uninfected targets upon the establishment of cell-cell contacts. This mechanism allows virus transmission via short and transient cell-cell interactions (Fig. 7; see also Movies S7 and S8 in the supplemental material). In contrast, we have recently demonstrated that prolonged cell-cell interactions that last longer than 30 min lead to polarized assembly, a process by which MLV assembly is directed toward sites of cell-cell contact (14). By studying MLV transmission using adherent fibroblasts as a model system, we have thus far characterized at least two distinct mechanisms of cell-to-cell transmission. Recent reports suggest that both of these mechanisms, surface-based transmission and *de novo* assembly at the site of contact, may also contribute to the spread of HIV among T cells (12, 26). The extent by which each mode of virus spread is used will likely depend on the expression level and affinity of receptor molecules in various cell types, the level of Env, and the nature and duration of cell-cell contacts.

ACKNOWLEDGMENTS

This study was supported by a grant from the National Cancer Institute (ROI CA098727) to W.M. N.M.S. received support from Long-term Fellowship ALTF 2007-176 from the European Molecular Biology Organization. J.J. is a recipient of a fellowship from the amfAR Foundation for AIDS research.

We are very grateful to Maik Lehmann, David Wensel, James Cunningham, Gary Nolan, Steven Goff, Johannes Huppa, and Michael Malim for sharing reagents and resources, and we thank Brett Pearson for a helpful discussion of the data.

REFERENCES

1. **Barnett, A. L., R. A. Davey, and J. M. Cunningham.** 2001. Modular organization of the Friend murine leukemia virus envelope protein underlies the mechanism of infection. Proc. Natl. Acad. Sci. U. S. A. **98:**4113–4118.
2. **Bourinbaiar, A. S., and D. M. Phillips.** 1991. Transmission of human immunodeficiency virus from monocytes to epithelia. J. Acquir. Immune Defic. Syndr. **4:**56–63.
3. **Cavrois, M., J. Neidleman, and W. C. Greene.** 2008. The Achilles heel of the Trojan horse model of HIV-1 trans-infection. PLoS Pathog. **4:**e1000051.
4. **Davey, R. A., C. A. Hamson, J. J. Healey, and J. M. Cunningham.** 1997. In vitro binding of purified murine ecotropic retrovirus envelope surface protein to its receptor, MCAT-1. J. Virol. **71:**8096–8102.
5. **Davis, H. E., J. R. Morgan, and M. L. Yarmush.** 2002. Polybrene increases retrovirus gene transfer efficiency by enhancing receptor-independent virus adsorption on target cell membranes. Biophys. Chem. **97:**159–172.
6. **Davis, H. E., M. Rosinski, J. R. Morgan, and M. L. Yarmush.** 2004. Charged polymers modulate retrovirus transduction via membrane charge neutralization and virus aggregation. Biophys. J. **86:**1234–1242.
7. **Endress, T., M. Lampe, J. A. Briggs, H. G. Krausslich, C. Brauchle, B. Muller, and D. C. Lamb.** 2008. HIV-1-cellular interactions analyzed by single virus tracing. Eur. Biophys. J. **37:**1291–1301.
8. **Eugenin, E. A., P. J. Gaskill, and J. W. Berman.** 2009. Tunneling nanotubes (TNT) are induced by HIV-infection of macrophages: a potential mechanism for intercellular HIV trafficking. Cell Immunol. **254:**142–148.
9. **Geijtenbeek, T. B., D. S. Kwon, R. Torensma, S. J. van Vliet, G. C. van Duijnhoven, J. Middel, I. L. Cornelissen, H. S. Nottet, V. N. KewalRamani, D. R. Littman, C. G. Figdor, and Y. van Kooyk.** 2000. DC-SIGN, a dendritic cell-specific HIV-1-binding protein that enhances trans-infection of T cells. Cell **100:**587–597.
10. **Goffinet, C., I. Allespach, S. Homann, H. M. Tervo, A. Habermann, D. Rupp, L. Oberbremer, C. Kern, N. Tibroni, S. Welsch, J. Krijnse-Locker, G. Banting, H. G. Krausslich, O. T. Fackler, and O. T. Keppler.** 2009. HIV-1 antagonism of CD317 is species specific and involves Vpu-mediated proteasomal degradation of the restriction factor. Cell Host Microbe **5:**285–297.
11. **Guibinga, G. H., A. Miyanohara, J. D. Esko, and T. Friedmann.** 2002. Cell surface heparan sulfate is a receptor for attachment of envelope protein-free retrovirus-like particles and VSV-G pseudotyped MLV-derived retrovirus vectors to target cells. Mol. Ther. **5:**538–546.
12. **Hubner, W., G. P. McNerney, P. Chen, B. M. Dale, R. E. Gordon, F. Y. Chuang, X. D. Li, D. M. Asmuth, T. Huser, and B. K. Chen.** 2009. Quantitative 3D video microscopy of HIV transfer across T cell virological synapses. Science **323:**1743–1747.
13. **Igakura, T., J. C. Stinchcombe, P. K. Goon, G. P. Taylor, J. N. Weber, G. M. Griffiths, Y. Tanaka, M. Osame, and C. R. Bangham.** 2003. Spread of HTLV-I between lymphocytes by virus-induced polarization of the cytoskeleton. Science **299:**1713–1716.
14. **Jin, J., N. M. Sherer, G. Heidecker, D. Derse, and W. Mothes.** 2009. Assembly of the murine leukemia virus is directed towards sites of cell-cell contact. PLoS Biol. **7:**e1000163.
15. **Johnson, D. C., and M. T. Huber.** 2002. Directed egress of animal viruses promotes cell-to-cell spread. J. Virol. **76:**1–8.
16. **Jolly, C., K. Kashefi, M. Hollinshead, and Q. J. Sattentau.** 2004. HIV-1 cell to cell transfer across an Env-induced, actin-dependent synapse. J. Exp. Med. **199:**283–293.
17. **Jouvenet, N., S. J. Neil, M. Zhadina, T. Zang, Z. Kratovac, Y. Lee, M. McNatt, T. Hatziioannou, and P. D. Bieniasz.** 2009. Broad-spectrum inhibition of retroviral and filoviral particle release by tetherin. J. Virol. **83:**1837–1844.
18. **Lehmann, M. J., N. M. Sherer, C. B. Marks, M. Pypaert, and W. Mothes.** 2005. Actin- and myosin-driven movement of viruses along filopodia precedes their entry into cells. J. Cell Biol. **170:**317–325.
19. **McDonald, D., L. Wu, S. M. Bohks, V. N. KewalRamani, D. Unutmaz, and T. J. Hope.** 2003. Recruitment of HIV and its receptors to dendritic cell-T cell junctions. Science **300:**1295–1297.
20. **Medeiros, N. A., D. T. Burnette, and P. Forscher.** 2006. Myosin II functions in actin-bundle turnover in neuronal growth cones. Nat. Cell Biol. **8:**215–226.
21. **Neil, S. J., S. W. Eastman, N. Jouvenet, and P. D. Bieniasz.** 2006. HIV-1 Vpu promotes release and prevents endocytosis of nascent retrovirus particles from the plasma membrane. PLoS Pathog. **2:**e39.
22. **Neil, S. J., T. Zang, and P. D. Bieniasz.** 2008. Tetherin inhibits retrovirus release and is antagonized by HIV-1 Vpu. Nature **451:**425–430.
23. **Phillips, D. M.** 1994. The role of cell-to-cell transmission in HIV infection. AIDS **8:**719–731.
24. **Pizzato, M., E. D. Blair, M. Fling, J. Kopf, A. Tomassetti, R. A. Weiss, and Y. Takeuchi.** 2001. Evidence for nonspecific adsorption of targeted retrovirus vector particles to cells. Gene Ther. **8:**1088–1096.
25. **Pizzato, M., S. A. Marlow, E. D. Blair, and Y. Takeuchi.** 1999. Initial binding of murine leukemia virus particles to cells does not require specific Env-receptor interaction. J. Virol. **73:**8599–8611.
26. **Rudnicka, D., J. Feldmann, F. Porrot, S. Wietgrefe, S. Guadagnini, M. C. Prevost, J. Estaquier, A. T. Haase, N. Sol-Foulon, and O. Schwartz.** 2009. Simultaneous cell-to-cell transmission of human immunodeficiency virus to multiple targets through polysynapses. J. Virol. **83:**6234–6246.
27. **Sattentau, Q.** 2008. Avoiding the void: cell-to-cell spread of human viruses. Nat. Rev. Microbiol. **6:**815–826.

28. **Schelhaas, M., H. Ewers, M. L. Rajamaki, P. M. Day, J. T. Schiller, and A. Helenius.** 2008. Human papillomavirus type 16 entry: retrograde cell surface transport along actin-rich protrusions. PLoS Pathog. **4:**e1000148.
29. **Sheetz, M. P., N. L. Baumrind, D. B. Wayne, and A. L. Pearlman.** 1990. Concentration of membrane antigens by forward transport and trapping in neuronal growth cones. Cell **61:**231–241.
30. **Sherer, N. M., M. J. Lehmann, L. F. Jimenez-Soto, C. Horensavitz, M. Pypaert, and W. Mothes.** 2007. Retroviruses can establish filopodial bridges for efficient cell-to-cell transmission. Nat. Cell Biol. **9:**310–315.
31. **Sherer, N. M., M. J. Lehmann, L. F. Jimenez-Soto, A. Ingmundson, S. M. Horner, G. Cicchetti, P. G. Allen, M. Pypaert, J. M. Cunningham, and W. Mothes.** 2003. Visualization of retroviral replication in living cells reveals budding into multivesicular bodies. Traffic **4:**785–801.
32. **Smith, J. L., D. S. Lidke, and M. A. Ozbun.** 2008. Virus activated filopodia promote human papillomavirus type 31 uptake from the extracellular matrix. Virology **381:**16–21.
33. **Sowinski, S., C. Jolly, O. Berninghausen, M. A. Purbhoo, A. Chauveau, K. Kohler, S. Oddos, P. Eissmann, F. M. Brodsky, C. Hopkins, B. Onfelt, Q. Sattentau, and D. M. Davis.** 2008. Membrane nanotubes physically connect T cells over long distances presenting a novel route for HIV-1 transmission. Nat. Cell Biol. **10:**211–219.
34. **Ugolini, S., I. Mondor, and Q. J. Sattentau.** 1999. HIV-1 attachment: another look. Trends Microbiol. **7:**144–149.
35. **Walker, S. J., M. Pizzato, Y. Takeuchi, and S. Devereux.** 2002. Heparin binds to murine leukemia virus and inhibits Env-independent attachment and infection. J. Virol. **76:**6909–6918.
36. **Yu, H. J., M. A. Reuter, and D. McDonald.** 2008. HIV traffics through a specialized, surface-accessible intracellular compartment during trans-infection of T cells by mature dendritic cells. PLoS Pathog. **4:**e1000134.
37. **Yueh, A., and S. P. Goff.** 2003. Phosphorylated serine residues and an arginine-rich domain of the Moloney murine leukemia virus p12 protein are required for early events of viral infection. J. Virol. **77:**1820–1829.
38. **Zhang, Y. J., T. Hatziioannou, T. Zang, D. Braaten, J. Luban, S. P. Goff, and P. D. Bieniasz.** 2002. Envelope-dependent, cyclophilin-independent effects of glycosaminoglycans on human immunodeficiency virus type 1 attachment and infection. J. Virol. **76:**6332–6343.